New Phytologist

Research

A transcription factor OsbHLH156 regulates Strategy II iron acquisition through localising IRO2 to the nucleus in rice

Shoudong Wang[1], Lin Li[1], Yinghui Ying[1], Jin Wang[1], Ji Feng Shao[2], Naoki Yamaji[2], James Whelan[3], Jian Feng Ma[2] and Huixia Shou[1]

[1]State Key Laboratory of Plant Physiology and Biochemistry, College of Life Sciences, Zhejiang University, Hangzhou, Zhejiang 310058, China; [2]Institute of Plant Science and Resources, Okayama University, Chuo 2-20-1, Kurashiki 710-0046, Japan; [3]ARC Centre of Excellence in Plant Energy Biology, Department of Animal, Plant and Soil Science, School of Life Science, La Trobe University, Melbourne, Victoria 3086, Australia

Author for correspondence:
Huixia Shou
Tel: +86 571 88206146
Email: huixia@zju.edu.cn

Received: *11 June 2019*
Accepted: *19 September 2019*

New Phytologist (2019)
doi: 10.1111/nph.16232

Key words: Fe deficiency, nuclear localisation, protein interaction, rice, transcription factor.

Summary

- Plants have evolved two strategies to acquire ferrous (Strategy I) or ferric (Strategy II) iron from soil. The iron-related bHLH transcription factor 2 (IRO2) has been identified as a key regulator of iron acquisition (Strategy II) in rice. However, its mode of action, subcellular localisation and binding partners are not clearly defined.
- Using RNA-seq analyses, we identified a novel bHLH-type transcription factor, OsbHLH156. The function of OsbHLH156 in Fe homeostasis was analysed by characterisation of the phenotypes, elemental content, transcriptome, interaction and subcellular localisation of OsbHLH156 and IRO2.
- *OsbHLH156* is primarily expressed in the roots and transcript abundance is greatly increased by Fe deficiency. Loss of function of O*sbHLH156* resulted in Fe-deficiency-induced chlorosis and reduced Fe concentration in the shoots under upland or Fe(III) supplied conditions. Transcriptome analyses revealed that the expression of most Fe-deficiency-responsive genes involved in Strategy II were not induced in the *osbhlh156-1* mutant. Furthermore, OsbHLH156 was required for nuclear localisation of IRO2.
- We conclude that OsbHLH156 is required for a Strategy II uptake mechanism in rice, partnering with a previously identified 'master' regulator IRO2. Mechanistically it is required for the nuclear localisation of IRO2.

Introduction

Iron (Fe) is an essential micronutrient in plants (Balk & Schaedler, 2014; Briat *et al.*, 2015). Although many soils are rich in Fe, low Fe availability is common, especially under aerobic conditions or when the soil is alkaline (Guerinot & Yi, 1994). Plants have evolved two strategies to optimise Fe acquisition and uptake (Guerinot & Yi, 1994; Walker & Connolly, 2008; Brumbarova *et al.*, 2015). Strategy I Fe acquisition is a reduction-based strategy and is used by all dicotyledonous plants and nongramineous monocots. In *Arabidopsis thaliana*, the process includes proton release into the rhizosphere mediated by the plasma membrane H^+-ATPase AHA2, reduction of the ferric Fe (Fe(III)) to the ferrous Fe (Fe(II)) by Fe(III)-chelate reductase FRO2, and Fe (II) uptake by iron-regulated transporter 1 (IRT1) (Korshunova *et al.*, 1999; Robinson *et al.*, 1999; Rogers *et al.*, 2000; Santi & Schmidt, 2009; Nishida *et al.*, 2011). By contrast, in gramineous plants, Fe is acquired via the Strategy II, known as the chelation-based strategy. This strategy requires the synthesis and secretion of mugineic acids (MAs) (Takagi, 1976; Ma & Nomoto, 1996), which belong to the chemical family phytosiderophores. The precursor of MAs is methionine synthesised through the Yang cycle (Ma *et al.*, 1995). Methionine that enters the MA biosynthetic pathway is first converted to *S*-adenosyl methionine, then to nicotianamine (NA) by NA synthase (NAS; Higuchi *et al.*, 1999), and finally to 2′-deoxymugineic acid (DMA) or other MAs (Takahashi *et al.*, 1999; Bashir *et al.*, 2006) by a two-step reaction mediated by NA aminotransferase (NAAT) and 2′-deoxymugineic acid synthase (DMAS). MAs is secreted into the soil, where they chelate Fe(III), mediated by TOM1 (Nozoye *et al.*, 2011). Fe(III)-MA complexes are transported into plant cells by the Yellow Stripe (YS) or YS-like transporters (YSL) (Curie *et al.*, 2001). Rice can use either Strategy I or II to uptake Fe(II) or Fe(III) depending on the growth conditions (Ishimaru *et al.*, 2006; Cheng *et al.*, 2007). Under flooded conditions, when Fe(II) is plentiful in the soil solution, rice employs a Strategy I-like approach to take up Fe(II) directly (Ishimaru *et al.*, 2006; Cheng *et al.*, 2007). By contrast, under upland soil conditions, much of the Fe is present in the insoluble form Fe(III), and acquisition relies on the MA-mediated Strategy II.

The regulation of Fe acquisition via Strategy I involves several members of the basic helix–loop–helix (bHLH) family. For instance, *FER* encoding a bHLH type of transcription factor, was first isolated from tomato by map-based cloning, the *fer* mutant

had a prominent chlorotic phenotype by contrast with wild-type plants (Ling *et al.*, 2002). The Fe-deficiency induced transcription factor (*FIT*) in Arabidopsis is orthologous to *FER*, and its expression was induced at the transcriptional and posttranscriptional levels by Fe limitation (Colangelo & Guerinot, 2004; Yuan *et al.*, 2005; Bauer *et al.*, 2007; Wu & Ling, 2019). FIT is essential for the induction of *AtFRO2* at the transcriptional level, and *AtIRT1* at both the transcriptional and posttranscriptional levels (Colangelo & Guerinot, 2004; Jakoby *et al.*, 2004). The activation of downstream signaling by FIT requires a number of binding partners in the Ib subgroup of bHLH transcription factors, namely AtbHLH38/39/100/101(Wang *et al.*, 2013; Yuan *et al.*, 2008).

The regulation of Fe acquisition via Strategy II is regulated by a different set of transcription factors, but is less understood compared with Strategy I. The iron-related bHLH transcription factor 2 (IRO2) was identified as a key regulator of Strategy II in rice, although its mode of action and subcellular localisation were not defined (Ogo *et al.*, 2006, 2007). IRO2 is induced by Fe limitation in roots and shoots and regulates the expression of phytosiderophore biosynthesis genes, including *OsNAS1*, *OsNAS2*, *OsNAAT1*, *OsDMAS1*, metallothionein-like gene *OsIDS1 and* the Fe(III)-DMA transporter *OsYSL15* (Inoue *et al.*, 2003; Cheng *et al.*, 2007). Two other transcription factors, iron deficiency-responsive element binding factors *OsIDEF1* and *OsIDEF2* are constitutively expressed and positively regulate a variety of genes in rice by binding to the iron deficiency-responsive *cis*-acting elements 1 (IDE1) and 2 (IDE2). OsIDEF1 positively regulates the expression of *IRO2,* thus sequentially controlling the majority of genes thought to be responsible for the Strategy II-based Fe acquisition. OsIDEF2 binds to the promoters of *OsYSL2* and several downstream genes of IRO2 (Kobayashi *et al.*, 2007; Ogo *et al.*, 2008). By contrast, OsIRO3, the orthologue of Arabidopsis AtPYE, is a negative regulator of Fe deficiency in rice (Zheng *et al.*, 2010).

In this study, we have identified a novel bHLH transcription factor, OsbHLH156, that regulates Fe acquisition specifically in Strategy II in rice. Functional analysis revealed that OsbHLH156 is required for induction of Fe-deficiency-responsive genes involved in Strategy II. Importantly, OsbHLH156 physically interacts with a major regulator IRO2, and facilitates its nuclear localisation during Fe deficiency in rice.

Materials and Methods

Plant materials and growth conditions

Rice plants (*Oryza sativa* L. cv Nipponbare) were used in this study. Seeds were germinated for 2 d before place on a net floating on nutrient solution. Nutrient solution was changed every 2 d. Plants were grown in a growth chamber at 30°C during the day and at 22°C during the night.

For the hydroponic experiments supplied with Fe (+Fe) or without Fe (−Fe), germinated seeds were placed on a culture solution containing 0.51 mM K_2SO_4, 1.64 mM $MgSO_4$, 0.32 mMNaH_2PO_4, 1.0 mM $CaCl_2$, 1.43 mM NH_4NO_3, 9 μM $MnCl_2$, 0.13 μM $CuSO_4$, 0.02 μM H_3BO_3, 0.08 μM $(NH_4)_6Mo_7O_{24}$, 0.15 μM $ZnSO_4$, 0.25 mM Na_2SiO_3 and 125 μM EDTA-Fe(II) (if supplied), pH 5.5–5.6. For hydroponic experiments supplied with different forms of Fe, 16-d-old wild-type and *osbhlh156-1* seedlings were grown in a nutrient solution containing either 20 μM Fe(II) as $FeSO_4$ or 20 μmol kg^{-1} Fe(III) as $Fe(OH)_3$. Plant growth was also assessed in plants grown in flooded or upland soil conditions with four replicates using 10-d-old seedlings prepared as described for the analysis of plants grown under different Fe levels. The plants were watered with tap water every day.

Plasmid construction for plant transformation

For the expression pattern assay, the 2225-bp sequence upstream ATG of *OsbHLH156* (the promoter of *OsbHLH156*) was amplified from wild-type genomic DNA with gene specific primers (Supporting Information Table S1) and cloned into pBI121 at the *Xba*I site to fuse to the *GUS* gene to generate the plasmid $P_{OsbHLH156}$::*GUS*. To generate the construct for the CRISPR/Cas9 system, a 20-bp target sequence of 5′-GCCGGCGTGTT CGCCGATGT-3′ at the first exon of *OsbHLH156* was used to design a gRNA spacer and fused to the U3 promoter at the *Bsa*I site of pRGE31 (Addgene, Watertown, MA, USA) as described (Xie *et al.*, 2014). For the complementation of the *osbhlh156-1* mutant, the 4424-bp genomic sequence of *OsbHLH156* was cloned into pTF101.1-ubi at the *Pst*I site to generate plasmid *pTF101-OsbHLH156* (Cheng *et al.*, 2007). The above constructs were introduced into *Agrobacterium* strain EHA101 or EHA105 for rice transformation of callus that was derived from mature seeds of wild-type via *Agrobacterium*-mediated transformation as described previously (Chen *et al.*, 2003).

Histochemical GUS assay

Germinated seeds were placed on a net that was floating on nutrient solution with or without Fe for 10 d. Fresh tissues were submerged in GUS-staining buffer, containing 10 mM Na_2EDTA, 1 mM$K_3[Fe(CN_6)]$, 1 mM $K_4[Fe(CN_6)]$, 100 mM sodium phosphate buffer, pH 7.0, 0.5% (v/v) Triton X-100, 20% (v/v) methanol, and 0.5 mg ml^{-1} 5-bromo-4-chloro-3-indolyl-D-glucuronic acid (X-gluc), vacuum infiltrated for 30 min, and incubated at 37°C overnight. The tissues were visualised under a stereoscope. Sections of 40 or 80 μm thickness were cut using a vibrating microtome (VT1000 S; Leica, Bensheim, Germany) and the images were examined under a microscope (Eclipse 90i; Nikon, Tokyo, Japan).

Transcription activation assay

Full-length cDNA of *OsbHLH156* was amplified and cloned into pGBKT7 vector (Clontech, Palo Alto, CA, USA) at the *Nde*I and *Pst*I sites, the generated plasmids *pBD-OsbHLH156* was then transformed into *Saccharomyces cerevisiae* AH109 (WEIDI, Shanghai, China) according to the manufacturer's instructions. The yeast colonies were streaked on SD (−Trp) plates with 40 mg l^{-1} 5-bromo-4-chloro-3-indoxyl-D-galactopyranoside

(X-α-Gal), which was used as substrate for detection of *lacZ* reporter gene activation. *pBD-OsIRO2* and empty *pGBKT7* vector (BD) were used as positive and negative control, respectively. Plates were incubated at 28°C for 4–6 d.

Determination of concentrations of elements in plants

For determination of element concentration in the shoots, samples were digested in 5 ml of 11 M HNO_3 for 5 h at 150°C. Element concentration was measured using an inductively coupled plasma mass spectrometry (ICP-MS; Agilent 7500ce, Palo Alto, CA, USA).

Global transcriptional comparison between wild-type and *osbhlh156-1* mutant

Wild-type and the *osbhlh156* mutant were grown in a nutrient solution with or without Fe for 10 d. Both the shoots and roots were harvested for RNA extraction as described above. Three biological replicates were used for each sample. The sequencing was performed at the Beijing Genomics Institute using the Illumina HiSeq platform. Adaptor-polluted, low-quality, unknown base (N), and counts below 20 reads per million were removed. The clean reads were mapped to reference using Bowtie 2 (http://bowtie-bio.sourceforge.net/bowtie2/index.shtml), and then calculate gene expression level using Rsem (RNA-seq by expectation maximization). Differentially expressed genes (DEGs) between samples were detected with DESeq2 (http://www.bioconductor.org/packages/release/bioc/html/DESeq2.html). The cutoff value, fragments per kilobase of transcript per million mapped reads (FPKM) > 10, $\log_2$(fold change) > 1 or < −1 with padj < 0.05, was used for DEG analysis. Venn2.1 (https://bioinfogp.cnb.csic.es/tools/venny/) software was used to display expressed genes between samples. The RNA-seq data were archived at NCBI under the accession no. PRJNA527175.

Quantitative RT-PCR

Total RNA was extracted from plants that had been grown with or without Fe for 10 d, using an RNA extraction kit (Tiangen Biotech, Beijing, China). A cDNA Synthesis Kit (TaKaRa, Dalian, China) was used to synthesise first-strand cDNA. Quantitative RT-PCR was performed using the SYBR Green Supermix system on a LightCycler 480 machine (Roche, Mannheim, Germany). *OsActin* was used as the internal control to normalise the samples. Primers are listed in Table S1. All experiments were performed in three biological and two technical replications.

Bimolecular fluorescence complementation (BiFC) assays and co-localisation of OsbHLH156 and IRO2

For the constructs used in BiFC assays, the coding sequences of *OsbHLH156* and *IRO2* were fused to the N-terminus of p2YN and p2YC vectors (Yang *et al.*, 2007), to generate the vectors *OsbHLH156-nYFP*, *OsbHLH156-cYFP*, *IRO2-nYFP* and *IRO2-cYFP*. The constructs were introduced into *Agrobacterium* strain EHA105. For co-localisation, the *OsbHLH156* CDS was cloned into vector *pSAT6-EYFP-C1* (http://www.bio.purdue.edu/people/faculty/gelvin/nsf/protocols_vectors.htm) to obtain a construct containing C-terminal yellow fluorescent protein (YFP) fusions, named *OsbHLH156-YFP*. The *IRO2* CDS was fused to the N-terminus of mCherry to generate the construct *IRO2-mCherry*. The *OsbHLH156-YFP* and *IRO2-mCherry* fragments were also introduced into *pCAMBIA1300* to observe the co-localisation of OsbHLH156 and IRO2 proteins in tobacco (*Nicotiana benthamiana*) leaves.

For preparing the protoplasts, rice seedlings were grown in the nutrient solution supplied with or without Fe with light for 1 wk and then in darkness for 1 week. Next, 1–2 mm sections of the stems and leaf sheaths were cut and transferred to lysis buffer for 30 min vacuum followed by 4 h incubation to prepare protoplasts. Rice protoplast transformation was performed as described previously (Wang *et al.*, 2019). Images were taken after incubation at 25°C in the dark for 12–15 h.

Tobacco plants were grown hydroponically in Hoagland medium for 2 wk and treated with or without Fe for 10 d. The corresponding constructs were transiently expressed in young leaves of tobacco by *Agrobacterium*-mediated infiltration method as described previously (Ying *et al.*, 2017). Images of tobacco leaf epidermal cells were taken 3 d after infiltration. The YFP and mCherry fluorescence signals in rice protoplasts and tobacco leaves were detected using a LSM710 NLO confocal laser scanning microscope (Zeiss).

Extraction of nuclear proteins

Nuclear proteins of tobacco leaves were extracted using nuclei isolation buffer and nuclei lysis buffer as described (Saleh *et al.*, 2008).

Co-IP assay

The coding sequences of *OsbHLH156* and *IRO2* were subcloned in frame into modified pCAMBIA1300 with 3Flag or 4Myc tags (Ying *et al.*, 2017) to generate *3Flag-OsbHLH156* and *4Myc-IRO2* constructs. The *3Flag-GFP* construct was used as a negative control. Tobacco leaves co-expressing *3Flag-OsbHLH156* (or *3Flag-GFP*) and 4Myc-IRO2 were sampled. Proteins were extracted using protein extraction buffer (50 mM Tris-HCl pH 7.5, 150 mM NaCl, 10% (v/v) glycerol, 0.1% (v/v) Nonidet P-40, 1 mM PMSF, and 1× protease inhibitor cocktail (Sigma-Aldrich, MO, USA). After centrifugation, the supernatant of cell lysate was incubated with anti-Flag® M2 magnetic beads (Sigma-Aldrich) at 4°C overnight and eluted according to the manufacturer's instructions. 3Flag-OsbHLH156/3Flag-GFP and 4Myc-IRO2 proteins were detected using anti-Flag (Sigma-Aldrich) and anti-Myc (Merck Millipore, Darmstadt, Germany) antibodies, respectively.

Accession numbers

Accession numbers of sequence data in this article are listed as follows:

Oryza sativa: IRO2 (*OsbHLH056*), LOC_Os01g72370; *OsPRI1* (*OsbHLH60*), LOC_Os08g04390; *OsbHLH062*, LOC_Os07g43530; *IRO3* (*OsbHLH063*), LOC_Os03g26210; *OsbHLH156*, LOC_Os04g31290. OsbHLH006, LOC_Os04g23550; OsbHLH009, LOC_Os10g42430; OsbHLH001, LOC_Os01g70310; *Arabidopsis thaliana: FIT*, AT2G28160; *PYE*, AT3G47640; *AtbHLH38*, AT3G56970; *AtbHLH39*, AT3G56980; *AtbHLH100*, AT2G41240; *AtbHLH101*, AT5G04150; *AtbHLH115*, AT1G51070. *Solanum lycopersicum: SlFER*, AAN39037.1.

Results

Identification of an Fe-deficiency-induced transcription factor OsbHLH156

To identify genes that potentially regulate Fe acquisition under Fe-deficient conditions, we conducted a RNA-sequence analysis of root and shoot of Nipponbare (a wild-type rice variety) seedlings. Seedlings were grown hydroponically in medium supplied with or without 125 μM EDTA-Fe for 10 d. Among the differentially regulated genes in response to Fe availability, we found a novel gene whose expression was dramatically induced by Fe deficiency in roots. The initial observation was confirmed by quantitative RT-PCR (qRT-PCR), in which the transcript abundance of the gene was induced 15-fold by Fe deficiency in the roots, but not in the shoots (Fig. 1a). The gene codes for an uncharacterised bHLH transcription factor, which was classified as OsbHLH156. Phylogenetic analysis revealed that OsbHLH156 belongs to the same clade as FIT and FER (Fig. 1b), but its amino acid sequence shares only 40% and 38.8-% similarity with that of FIT and FER, respectively (Fig. S1).

Although *OsbHLH156* was previously reported as a *OsFER*-like gene, it was not detected in EST libraries, and was assumed to have little to no expression (Ogo *et al.*, 2006). Moreover, *OsbHLH156* was not included in the Affymetrix Rice Gene Chip (Cheng *et al.*, 2007), therefore its expression was not detected in previous studies on Fe responses in rice (Ogo *et al.*, 2006; Cheng *et al.*, 2007). To determine the expression pattern of *OsbHLH156*, we fused the 2225-bp region upstream of *OsbHLH156* coding region to the β-glucuronidase (GUS) encoding gene to form the $P_{OsbHLH156}$:*GUS* construct. Under normal Fe supply conditions, GUS activity was detected only in the meristematic zone of lateral and primary roots (Fig. 1c). However, when plants were grown in Fe-deficient media, GUS staining was clearly detected in whole roots, especially in the meristematic zone (Fig. 1c). Cross-sections of the GUS-stained roots grown in Fe-deficient conditions showed that GUS expression was observed throughout the roots, including the epidermis, exodermis, cortex, endodermis and the stele of the maturation zone (Fig. 1d). The expression pattern was similar to that of IRO2 (Ogo *et al.*, 2011).

To assess the subcellular localisation of OsbHLH156, the full-length coding sequence of *OsbHLH156* was fused to the N-terminus of YFP and transiently expressed in rice protoplasts. The YFP signal of OsbHLH156-YFP was detected in the nucleus (Fig. 1e). In this assay, YFP alone resulted in diffuse distribution of fluorescence throughout the cell, including the cytoplasm and nucleus (Fig. 1e).

To determine whether OsbHLH156 has transcriptional activation, a plasmid that expressed a polypeptide consisting of OsbHLH156 fused to the GAL4 DNA-binding domain (GAL4BD) was transferred into yeast strain AH109. Yeast cells containing the GAL4BD-OsbHLH156 construct formed blue colonies, which was the same as the positive control for GAL4BD-OsIRO2 (Fig. 1f). The results demonstrated that OsbHLH156 possessed transcription activation ability.

Loss of *OsbHLH156* function results in enhanced sensitivity to Fe deficiency

To test the biological role of OsbHLH156 in Fe uptake and metabolism, we generated *osbhlh156* knockout mutants using the CRISPR/Cas9 system. The knockout line *osbhlh156-1* had a 'GA' deletion in the *OsbHLH156* coding region, which resulted in a frame-shift mutation after Ala37 (Figs 2a, S2). When grown on normal hydroponic medium supplied with 125 μM EDTA-Fe(II) as the Fe source, there were no obvious phenotypic changes in the *osbhlh156-1* mutant seedlings compared with the wild-type plants, except that root length of *osbhlh156-1* mutant was decreased (Fig. 2b–d). By contrast, when plants were grown on Fe-deficient medium, the leaves of the *osbhlh156-1* mutants were more chlorotic than wild-type plants, especially in young leaves that emerged under Fe-depleted conditions (Fig. 2b). The chlorophyll content of Fe-depleted *osbhlh156* mutants grown in Fe-depleted condition was decreased by 55% compared with the wild-type based on the Soil Plant Analysis Development (SPAD) value (Fig. 2d).

To test whether the chlorotic phenotype was due to altered Fe content, we measured and compared shoot Fe concentration of *osbhlh156-1* with wild-type plants. Under Fe-replete and Fe-deplete conditions, the shoot Fe concentration of *osbhlh156-1* was decreased by 33% and 27% compared with wild-type, respectively (Fig. 2e). Two additional CRISPR/CAS9 knockout lines, *osbhlh156-2* and *osbhlh156-3,* from the Zhonghua 11 genotype were obtained from the Biogle Genome Editing Center (http://www.biogle.cn/). Both *osbhlh156-2* and *osbhlh156-3* have an early termination of translation of OsbHLH156 (Fig. S2). These lines showed similar leaf chlorosis and reduced Fe concentration when grown in Fe deprivation conditions (Fig. S3). The chlorosis and reduced Fe concentration level of *osbhlh156-1* were restored by introducing the genomic DNA sequence of *OsbHLH156* (Fig. 2b–e), confirming that the mutant phenotypes were caused by disruption of the *OsbHLH156* gene.

Mutation in *OsbHLH156* suppressed expression of a great number of Strategy II Fe deficiency-responsive genes

To determine genes regulated by OsbHLH156, we performed RNA sequencing (RNA-seq) analyses of the shoots and roots of wild-type and *osbhlh156-1* plants grown in medium with or without an Fe supply. In *osbhlh156-1* roots, the expression of 2904 transcripts (1245 upregulated and 1659 downregulated)

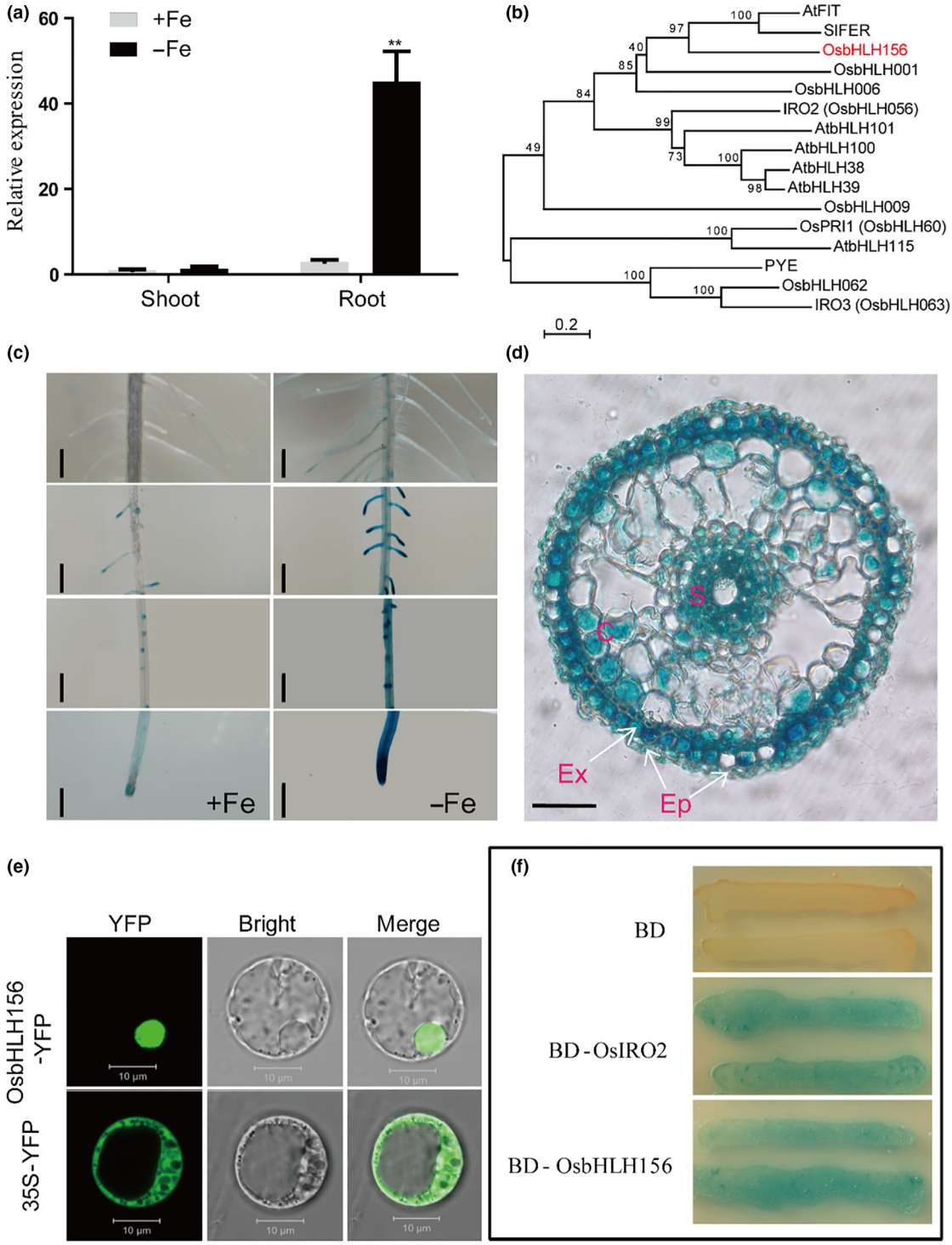

Fig. 1 Expression and localisation of OsbHLH156. (a) Relative transcript abundance of *OsbHLH156* in shoots and roots of rice seedlings grown with 125 μM EDTA-Fe(II) (+Fe) or no Fe (−Fe) for 10 d. Data represent means ± SD, $n = 3$; **, $P < 0.01$; one-way analysis of variance (ANOVA) followed by Tukey test. (b) Phylogenic analysis of OsbHLH156 protein and other bHLHs involved in Fe-deficiency response. Amino acid sequences of FIT protein were used to BLAST the rice genome and the retrieved top four proteins, OsbHLH156, OsbHLH001, OsbHLH006 and OsbHLH009, were included in the phylogenetic tree. This tree was constructed through the neighbour-joining method using MEGA 6.0 (https://www.megasoftware.net/reltime). (At, *Arabidopsis thaliana*; Os, *Oryza sativa*; Sl, *Solanum lycopersicum*). (c) β-Glucuronidase (GUS) staining of transgenic plants expressing $P_{OsbHLH156}$:*GUS* construct. Seedlings were grown with 125 μM EDTA-Fe(II) (+Fe) or no Fe (−Fe) for 10 d before the GUS-staining. Bars, 500 μm. (d) Cross-section of GUS-stained root (2–3 cm from the root tip) under Fe deficiency in (c). S, stele; C, cortex; Ex, exodermis; Ep, epidermis. Bar, 100 μm. (e) Subcellular localisation of OsbHLH156 in rice protoplasts. Yellow fluorescent protein (YFP) was fused to the C-terminus of OsbHLH156 and driven by a 35S CaMV promoter. Bars, 10 μm. (f) Transcription activation assay of OsbHLH156 and OsIRO2 in yeast. OsbHLH156 and OsIRO2 fused with GAL4 binding domain were expressed in *Saccharomyces cerevisiae* AH109. The blue colonies indicated that reporter gene *lacZ* was activated. The empty vector (BD) was used as negative control.

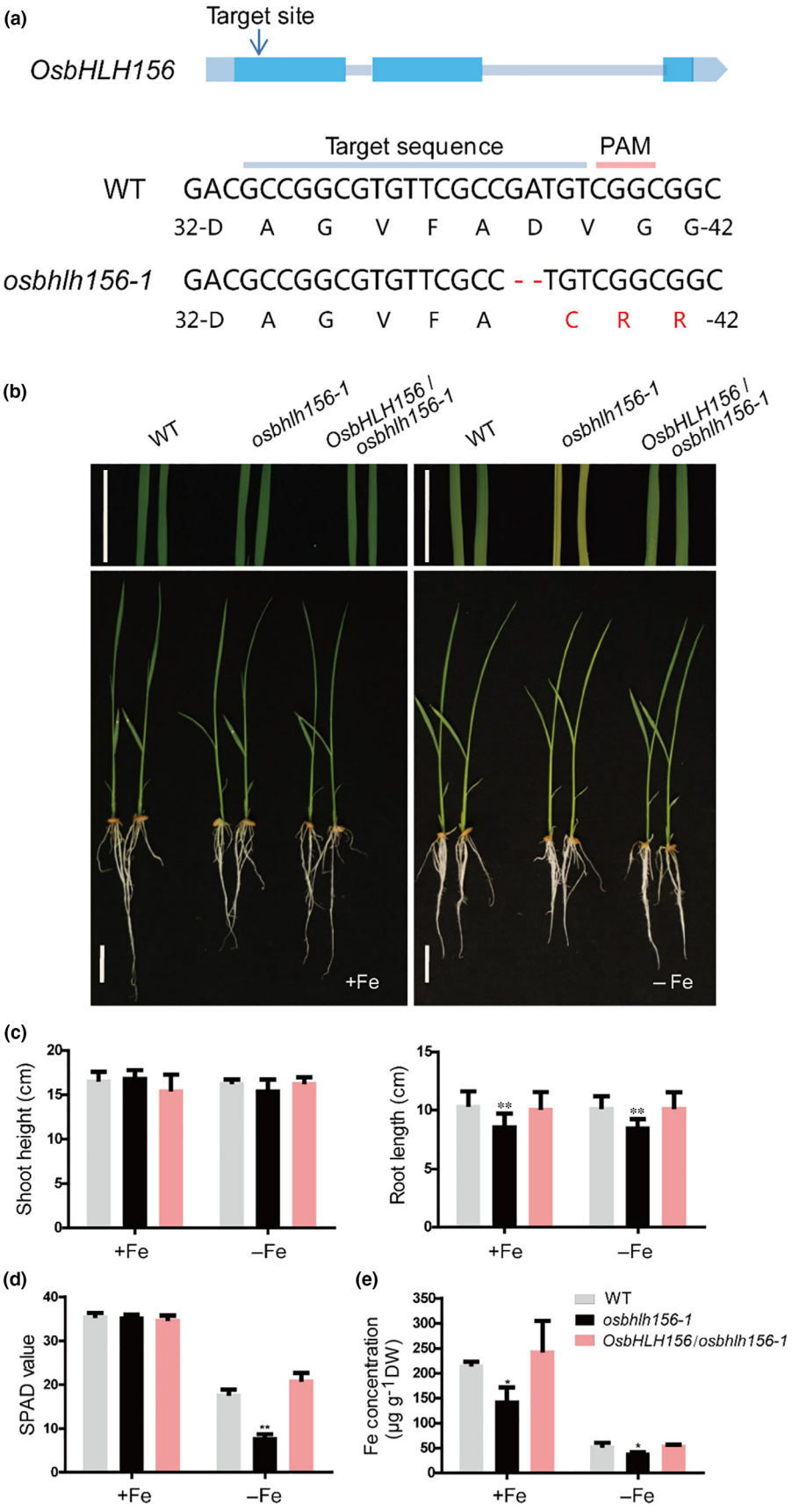

Fig. 2 Characteristics of the wild-type rice (WT), *osbhlh156-1* and complementation line grown under Fe-deficient and Fe-sufficient conditions. (a) Target site and sequence of *osbhlh156-1* for CRISPR/Cas9 mutation. The 20-nucleotide-leading sequence of gRNA (target sequence) and the protospacer-adjacent motif (PAM) are marked with blue and red lines, respectively. (b) Growth performance of WT, *osbhlh156-1* and the complementation line under hydroponic media supplied with 125 μM EDTA-Fe(II) (+Fe) or no Fe (–Fe). Bars, upper panels, 1 cm. Bars, lower panels, 3 cm. (c) Shoot heights and root lengths of WT, *osbhlh156-1* and the complementation line. (d) SPAD values representing chlorophyll content of leaves. (e) Shoot Fe content. Data are shown as the mean and SD ($n = 3$). Significance of differences compared with WT is indicated by asterisks. One-way ANOVA followed by Tukey test; *, $P < 0.05$; **, $P < 0.01$.

was altered by Fe deficiency (Fig. 3a; Table S2a) whereas in the wild-type roots only 653 transcripts were upregulated or down-regulated by Fe deficiency (442 up- and 211 down-regulated) (Fig. 3a; Table S2b). This difference in the number of induced transcripts cannot be attributed to the 'background' changes in *osbhlh156-1* as, under Fe-replete conditions, only 103 transcripts were differentially expressed in the roots of *osbhlh156-1* and wild-type plants (Fig. 3a; Table S2c). However, under Fe-deplete conditions, the differentially expressed transcripts reached 2703 (Fig. 3a; Table S2d), < 10% of the genes overlapped between the wild-type and mutant (Fig. S4). A similar pattern was observed in the shoots, but the response was clearly 3–5 times smaller in magnitude in both the wild-type and *osbhlh156-1* plants (Fig. 3a; Table S2e–h).

Among the 442 Fe-deficiency-induced transcripts in wild-type roots, 259 were significantly lower in *osbhlh156-1* than in wild-type (Table S3a). These groups of genes included those encoding HRZ2 (Haemerythrinmotif-containing Really Interesting New Gene and Zinc-finger protein), an orthologue of Arabidopsis BRUTUS that was proposed to be involved in Fe sensing (Kobayashi *et al.*, 2013), the Fe (II) transporter IRT1 (Bughio *et al.*, 2002), Fe(III)-DMA transporters YSL15 and 16 (Inoue *et al.*, 2009), NA aminotransferase NAAT1 (Cheng *et al.*, 2007; Lee *et al.*, 2012), NA efflux transporters ENA1 and 2 (Nozoye *et al.*, 2011), the DMA synthesis enzymes NAS1, 2, and 3 (Inoue *et al.*, 2003), DMAS1 (Bashir *et al.*, 2006), the DMA efflux transporter TOM1 (Nozoye *et al.*, 2011), and the transcription factor *bHLH133* (Wang *et al.*, 2013; Fig. S5; Tables 1, S3a). Similarly, among the 211 Fe-deficiency-suppressed transcripts in wild-type roots, there was also a group of 62 transcripts whose expression was significantly higher in *osbhlh156-1* than in the wild-type (Table S3b). These gene expression responses to Fe deficiency between wild-type and *osbhlh156-1* are summarised in the heatmap shown in Fig. 3(b).

We compared the transcript abundance of genes related to the Fe deficiency response in the roots of the wild-type and *osbhlh156-1* plants. Genes involved in Strategy I acquisition showed a similar response to Fe deficiency between wild-type and mutant plant although the induction differed to some extent (Table 1). By contrast, the expression of 22 genes involved in Strategy II Fe acquisition including MA synthesis, *S*-adenosylmethionine cycle and transporters was highly induced by Fe deficiency in wild-type, but not or hardly induced in *osbhlh156-1*. Interestingly, the expression of two transcriptional regulators *IRO2* and *IRO3* was induced by Fe deficiency in both the wild-type and *osbhlh156-1* plants (Table 1).

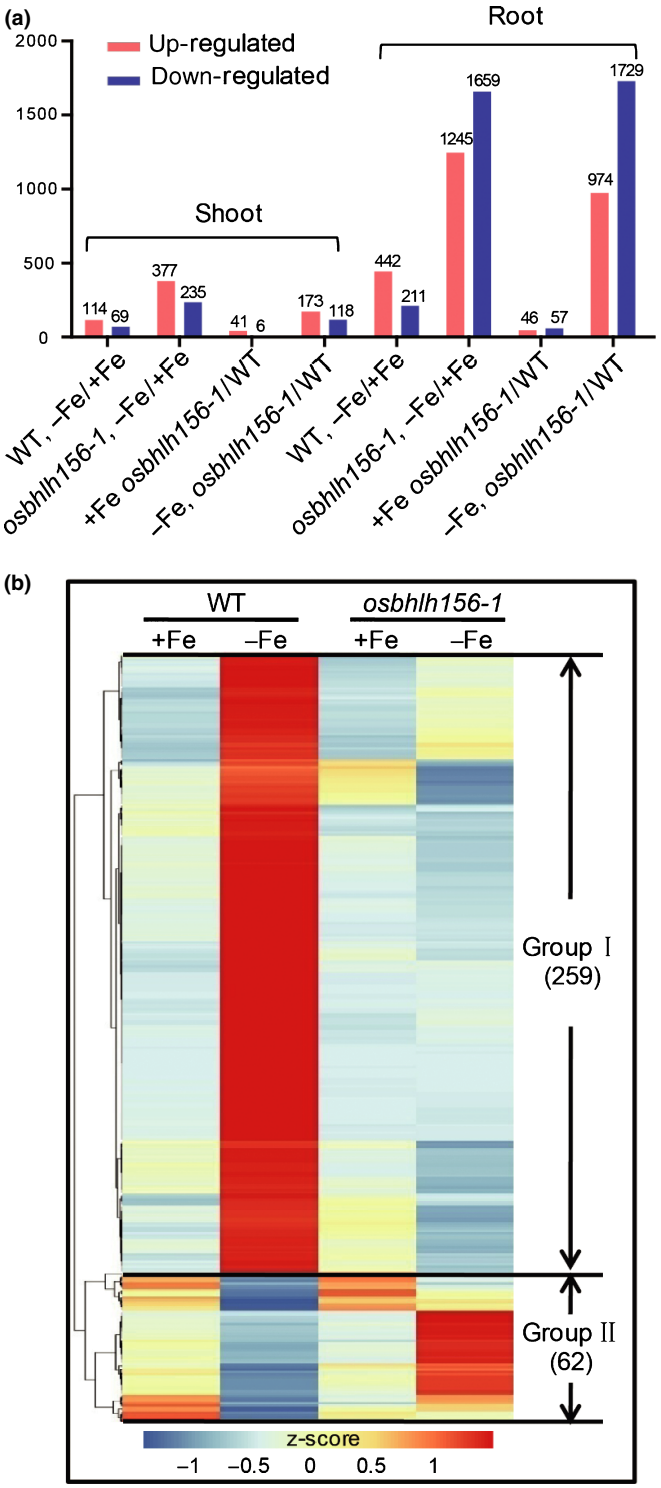

Fig. 3 Fe-deficiency-induced differential gene expression in wild-type (WT) rice and *osbhlh156-1*. (a) Number of different expressed transcripts under Fe deficiency in shoots and roots. Transcripts were screened for FPKM > 10. A significant fold change was defined as $\log_2$(fold change) > 1 or < −1 with a false discovery rate correction adjusted $P < 0.05$. (b) Heatmap. Note that the genes responded in an antagonistic manner in rice roots under Fe-deficiency condition. The colour scale shows the *z*-score associated with 321 genes. Group I consisted of 259 Fe-deficiency-induced transcripts, the expression of which was lower in *osbhlh156-1* than in the WT, while Group II includes 62 Fe-deficiency-suppressed genes, the expression of which was higher in *osbhlh156-1* than in the WT.

OsbHLH156 is involved in Strategy II Fe acquisition system

To test whether OsbHLH156 affects Strategy I or II of Fe acquisition, we grew wild-type and *osbhlh156-1* plants under flooded and upland conditions. Under flooded soil conditions, *osbhlh156-1* and wild-type plants grew similarly (Fig. 4). By contrast, under upland soil conditions, the *osbhlh156-1* mutant displayed impaired growth, leaf chlorosis (Fig. 4a) and decreased SPAD value (Fig. 4b), as well as a reduced Fe concentration in

Table 1 FPKM values for genes involved in Strategies I and II Fe acquisition in roots of wild-type rice (WT) and *osbhlh156-1*. The FPKM values were obtained from average of three biological replicates.

			WT		*osbhlh156-1*	
Gene locus	Gene name	Function	+Fe	−Fe	+Fe	−Fe
Genes involved in Strategy I Fe acquisition						
LOC_Os03g37490.1	*PEZ1*	Phenolics efflux transporter	3.9	1.4	4.3	1.5
LOC_Os03g37640.1	*PEZ2*	Phenolics efflux transporter	26.3	44.3	26.8	29.3
LOC_Os03g46470.1	*IRT1*	Fe(II) transporter	2.8	62.4	2.2	22.7
LOC_Os03g46454.1	*IRT2*	Fe(II) transporter	0.8	131.3	1.1	107.0
LOC_Os07g15460.1	*NRAMP1*	Fe(II) transporter	3.5	135.2	4.8	127.5
Genes involved in Strategy II Fe acquisition						
Genes encoding enzymes in DMA synthesis						
LOC_Os03g19427.1	*NAS1*	Nicotianamine synthase	48.1	5355.4	0.0	7.2
LOC_Os03g19420.2	*NAS2*	Nicotianamine synthase	56.0	6358.0	0.0	8.3
LOC_Os07g48980.1	*NAS3*	Nicotianamine synthase	16.3	64.7	25.1	13.1
LOC_Os02g20360.1	*NAAT1*	Nicotianamine aminotransferase	28.1	1279.1	4.3	22.1
LOC_Os03g13390.2	*DMAS1*	Deoxymugineic acid synthase	30.4	1030.2	8.7	18.3
Genes encoding enzymes in Yang cycle						
LOC_Os06g02220.1	*MTN*	Methylthioadenosine/S-adenosyl homocysteine nucleosidase	33.0	278.8	28.7	19.0
LOC_Os12g39860.1	*APT1*	Adenine phosphoribosyltransferase	111.2	852.0	92.9	66.4
LOC_Os04g57400.1	*MTK1*	Methylthioribose kinase	53.0	550.0	45.7	28.2
LOC_Os04g57410.1	*MTK2*	Methylthioribose kinase	9.6	152.6	7.6	4.6
LOC_Os11g11050.1	*IDI2*	Methylthioribose-1-phosphate isomerase	12.2	157.5	11.0	6.7
LOC_Os11g29370.1	*DEP*	Methylthioribulose-1-phosphate dehydratase-enolase-phosphatase	27.0	546.4	19.8	15.7
LOC_Os03g06620.1	*IDI1*	Acireductone dioxygenase	56.7	562.2	38.7	35.8
LOC_Os06g29180.1	*FDH*	Formate dehydrogenase	35.1	1040.9	33.1	56.4
LOC_Os09g28050.1	*IDI4*	Aminotransferase catalysing the synthesis	47.1	1037.9	36.4	29.6
LOC_Os05g04510.1	*SAM1*	*S*-adenosyl-L-methionine synthetase	919.5	874.6	712.6	491.1
LOC_Os01g22010.1	*SAM2*	*S*-adenosyl-L-methionine synthetase	740.2	2807.0	661.9	345.6
LOC_Os12g38270.1	*IDS1*	Dioxygenases catalysing the hydroxylation of MAs	502.3	3322.6	243.4	475.0
LOC_Os04g24140.1	*RPI*	Ribose-5-phosphate isomerase	28.4	465.1	17.9	72.3
Genes encoding transporters						
LOC_Os02g43410.1	*YSL15*	Fe(III)-DMA transporter	11.8	859.4	0.1	2.9
LOC_Os04g45900.1	*YSL16*	Fe(III)-DMA transporter	43.4	78.8	36.4	11.3
LOC_Os11g04020.1	*TOM1*	DMA efflux transporter	13.0	751.2	2.3	2.8
LOC_Os11g05390.1	*ENA1*	NA efflux transporter	4.9	57.2	0.5	0.6
LOC_Os06g48060.1	*ENA2*	NA efflux transporter	18.9	47.5	17.1	14.6
Genes encoding transcription factors						
LOC_Os01g72370.2	*IRO2*	Positive transcriptional regulator	9.4	530.7	17.2	686.3
LOC_Os04g31290.1	*OsbHLH156*	Positive transcriptional regulator	26.2	208.8	14.7	45.2
LOC_Os03g26210.2	*IRO3*	Negative transcriptional regulator	1.3	27.6	1.4	20.4

shoots, compared with wild-type plants (Fig. 4c). Furthermore, the growth of the wild-type and *osbhlh156-1* mutant was compared in the presence of Fe(II) ($FeSO_4$) or Fe(III) ($Fe(OH)_3$). When supplied with Fe(II), the wild-type and mutant plants grew similarly (Fig. 4d–f), but when supplied with Fe(III), *osbhlh156-1* plants showed chlorosis in the young leaves, while leaves of the wild-type plants were normal. These results indicated that the *osbhlh156-1* mutant is competent in taking up Fe as Fe(II), but not as Fe(III).

The transcription factor OsbHLH156 interacts with IRO2

The expression profile showed that the genes regulated by IRO2 failed to respond to Fe deficiency in *osbhlh156-1* mutant (Table 1). It is known that the bHLH proteins are a superfamily of transcription factors that binds as dimers to specific DNA target sites. In Arabidopsis, FIT protein interacts with the bHLH Ib proteins bHLH38/39/100/101 (Wang *et al.*, 2013; Yuan *et al.*, 2008). Therefore, we hypothesised that OsbHLH156, the FIT orthologue, may interact with the bHLH Ib family protein IRO2. To investigate this hypothesis, we first performed BiFC assays in tobacco leaf epidermal cells. As shown in Fig. 5(a), OsbHLH156 not only interacted with IRO2, but also formed a homodimer itself. Furthermore, we tested whether the two proteins could be co-immunoprecipitated. OsbHLH156 and IRO2 were tagged with 3Flag and 4Myc at their N-termini, respectively and transiently expressed in tobacco leaves, using 3Flag-GFP as a negative control. The 3Flag-OsbHLH156 and the putative interacting partners were co-immunoprecipitated using magnetic beads carrying anti-Flag antibodies. Co-immunoprecipitated 4Myc-IRO2 was detected using anti-Myc antibodies (Fig. 5b), therefore OsbHLH156 and IRO2 interact physically.

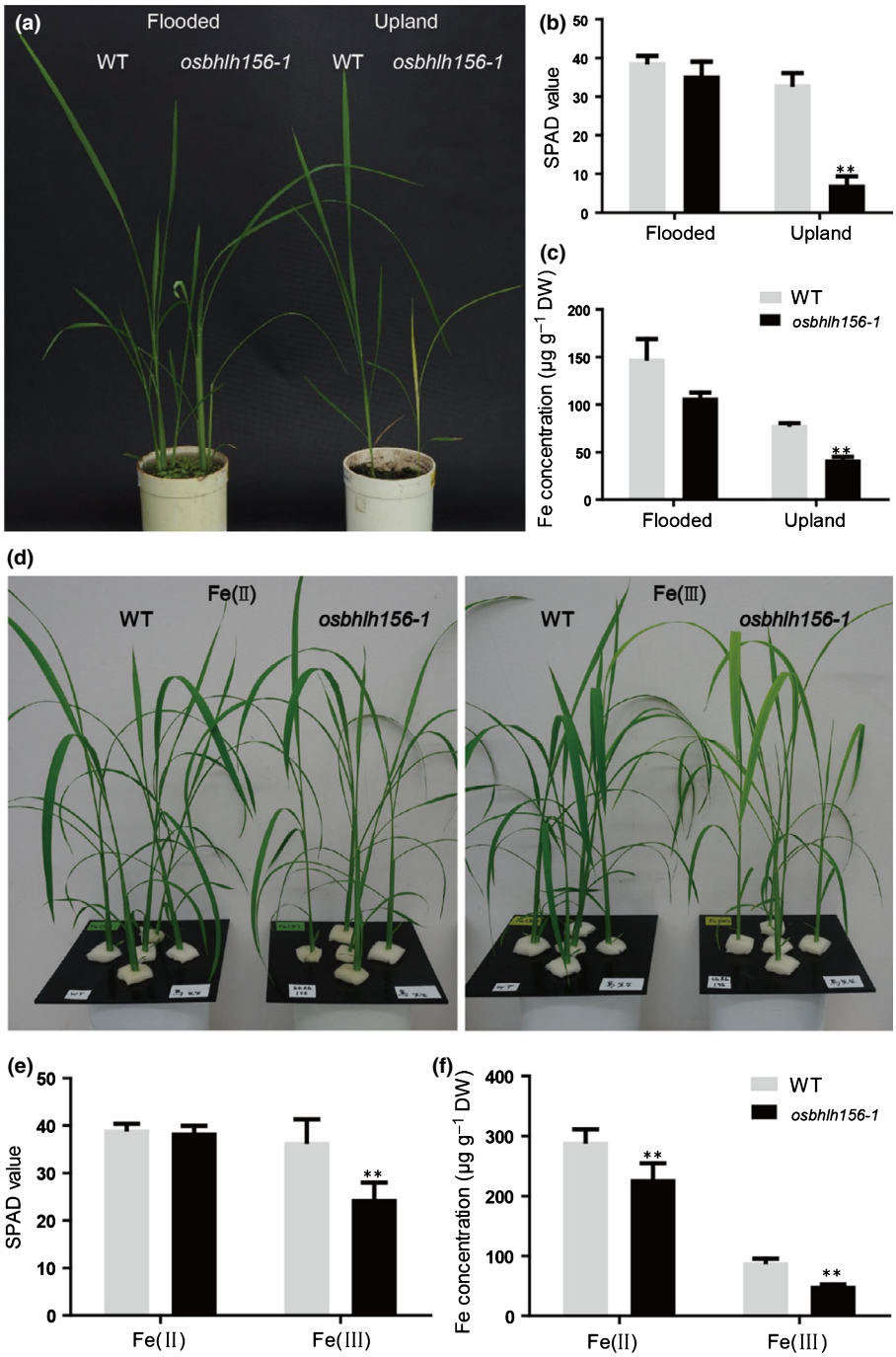

Fig. 4 Growth performance, leaf chlorophyll, and shoot Fe concentrations of wild-type rice (WT) and *osbhlh156-1* plants grown in different chemical forms of Fe supply. Growth performance (a), SPAD values (b) and shoot Fe content (c) of wild-type and *osbhlh156-1* mutant grown under flooded or upland conditions for 26 d. DW, dry weight; data represent means ± SD, $n = 4$; **, $P < 0.01$, one-way ANOVA followed by Tukey test. Growth performance (d), SPAD values (e) and shoot Fe content (f) of wild-type and *osbhlh156-1* mutant grown in Fe (II), supplied as $FeSO_4$ or Fe(III), supplied as $Fe(OH)_3$, for 11 d. DW, dry weight; data represent means ± SD, $n = 5$; **, $P < 0.01$; one-way ANOVA followed by Tukey test.

OsbHLH156 determines the nuclear localisation of IRO2

Although IRO2 was observed to interact with itself, the majority of the fluorescence signal was detected outside the nucleus (Fig. 5a). When IRO2 was co-expressed with OsbHLH156, a clear nuclear localisation was observed (Fig. 5a). This suggests OsbHLH156 may play a role in regulating the Fe-deficiency response by controlling the nuclear localisation of IRO2. To test this hypothesis, OsbHLH156-YFP, IRO2-mCherry and mCherry-IRO2 were transiently expressed in tobacco leaves separately or together. Under Fe-sufficient conditions, when expressed by themselves, OsbHLH156 was located in the nuclei, while IRO2 was mainly located in the cytoplasm (Fig. 6a). When both proteins were expressed together, the signal was mainly detected in the nucleus (Fig. 6a). Under Fe-limiting conditions, IRO2-mCherry was found to be, at least partially, localised in the nucleus.

We next tested the effects of Fe deficiency on IRO2 localisation by immunoblotting of nuclear fraction of transfected tobacco leaves (Fig. 6b). Nuclear protein was extracted and quality-controlled using Histone H3 as a marker of nuclear protein and co-infiltrated GFP as a loading control. Under Fe-sufficient conditions, expression of 4Myc-IRO2 alone resulted in a comparatively low

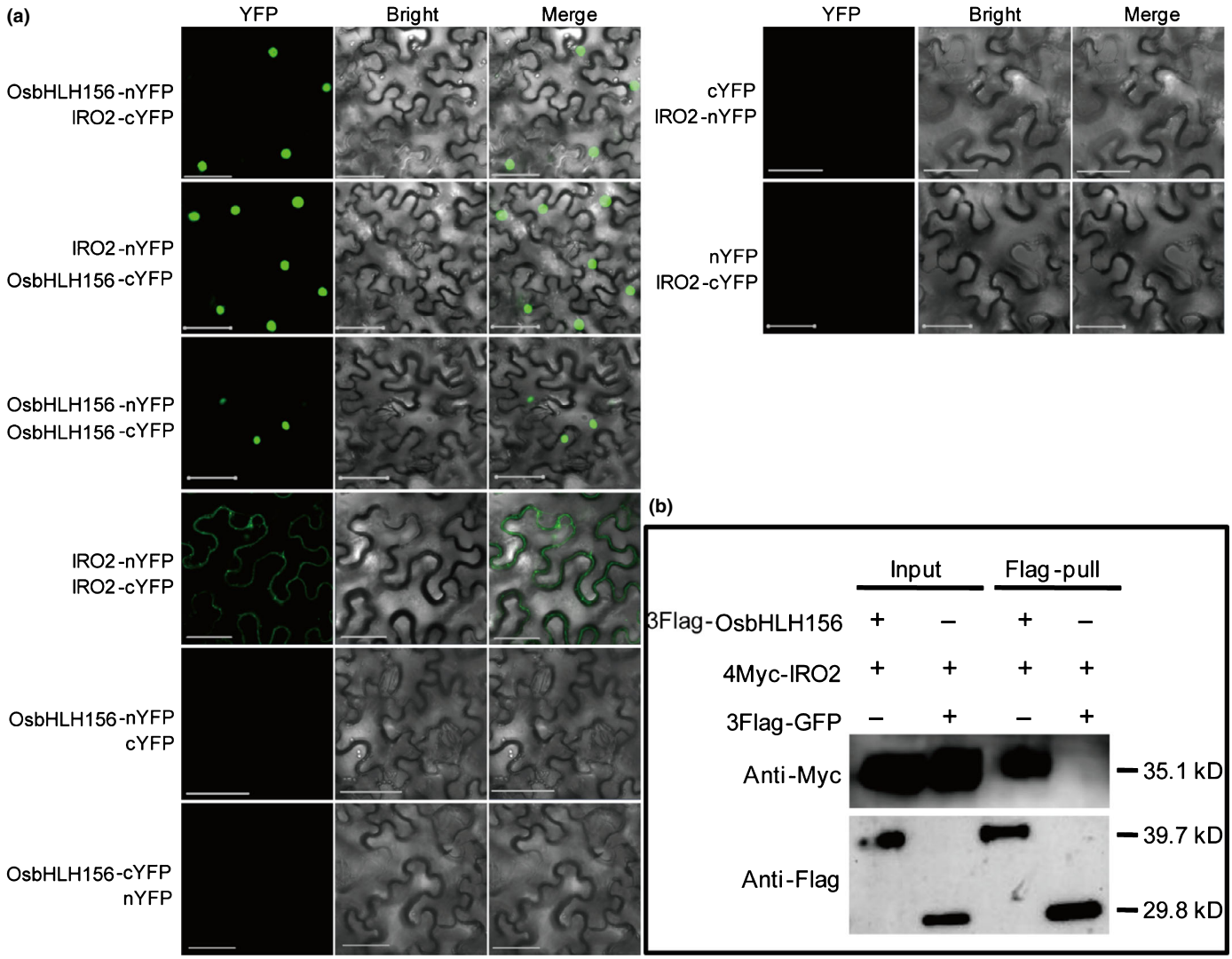

Fig. 5 Interaction of OsbHLH156 and IRO2. (a) Bimolecular fluorescence complementation of OsbHLH156 and IRO2. OsbHLH156 and IRO2 were fused to the N- or C-terminus of yellow fluorescent protein (namely nYFP or cYFP) and transiently expressed in tobacco leaf epidermal cells. The ability to form both homodimers and heterodimers was tested using different combinations. Bars, 50 μm. (b) Co-immunoprecipitation (Co-IP) of OsbHLH156-IRO2 in tobacco leaves. The 3Flag tag was fused to the N-terminus of OsbHLH156 and green fluorescent protein (GFP; as a control for pull-down). The 4Myc tag was fused to N-terminus of IRO2. The molecular mass of proteins is shown in kDa. The molecular masses at 35.1 kDa, 39.7 kDa and 29.8 kDa correspond to 4Myc-IRO2, 3Flag-OsbHLH156 and 3Flag-GFP, respectively.

amount of IRO2 protein in the nuclear fraction (lane 1 in Fig. 6b). However, under Fe-deficiency conditions, the amounts of IRO2 accumulated in the nucleus were significantly increased (lane 3 in Fig. 6b). When IRO2 was co-expressed with 3Flag-OsbHLH156, a strong signal was detected for IRO2 protein in the nuclear protein extract of tobacco leaves from both Fe-replete or Fe-deplete conditions (lane 2 and lane 4 in Fig. 6b).

The interaction between OsbHLH156 and IRO2 was further confirmed in rice leaf protoplasts derived from *osbhlh156-1* seedlings grown in both Fe-supplied or Fe-deplete conditions. Results showed that nuclear localisation required the presence of OsbHLH156 in both under Fe-replete or Fe-deplete conditions. Co-expression of OsbHLH156-YFP and IRO2-mCherry resulted in nuclear localisation of IRO2 (Figs 6c, S6).

Discussion

In the study, we demonstrated that a novel transcription factor, OsbHLH156, is involved in the regulation of Strategy II Fe acquisition by partnering with the Strategy II master regulator IRO2. This conclusion is supported by the following key evidence:

(**1**) Expression of *OsbHLH156* is induced by Fe deficiency in the roots, similar to *IRO2* (Fig. 1a, c).

(**2**) Knockout of *OsbHLH156* resulted in chlorosis and decreased Fe concentration in leaves when grown under upland soil conditions, in which the available Fe is in the form of Fe(III) or Fe(III) supplied in hydroponic solution, but not in flooded or Fe(II) supplied conditions (Fig. 4).

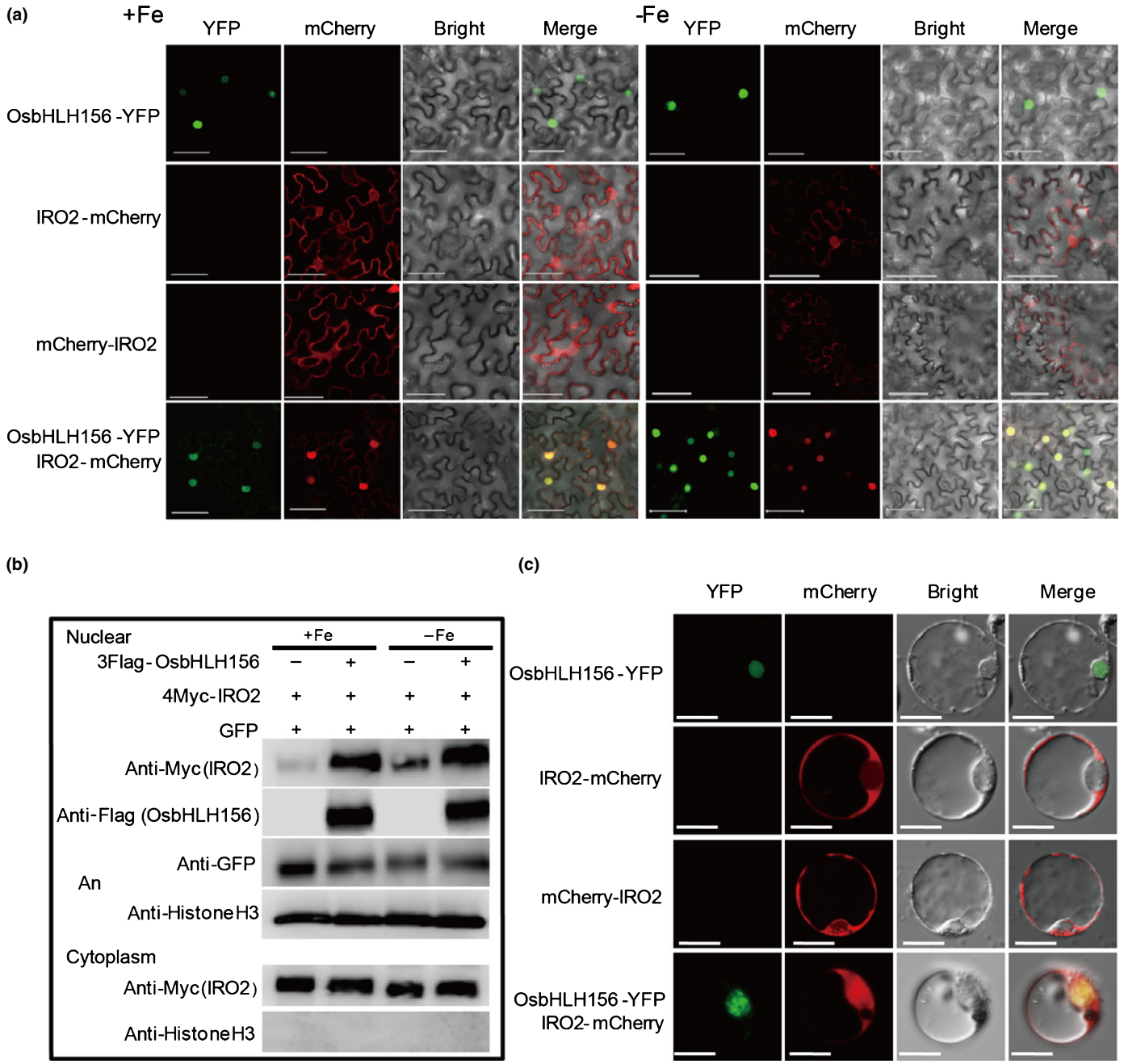

Fig. 6 Nuclear localisation of IRO2 requires OsbHLH156. (a) Co-localisation of OsbHLH156 and IRO2 in epidermal cells. OsbHLH156-YFP, IRO2-mCherry and mCherry-IRO2 were expressed separately or together in new leaves of tobacco that were grown with or without Fe. Bars, 50 μm. (b) Immunoanalyses of proteins in the nuclear fraction of tobacco leaves that transiently expressed IRO2 alone or co-expressed OsbHLH156 with IRO2. GFP was co-infiltrated as a loading control, and Histone H3 was used as a marker of nuclear protein. (c). Co-localisation of OsbHLH156 and IRO2 in the nucleus of rice protoplasts prepared from rice seedlings grown under Fe-replete conditions. OsbHLH156-YFP, IRO2-mCherry and mCherry-IRO2 were expressed separately or together in leaf protoplasts that were isolated from *osbhlh156-1* seedlings grown in Fe-deplete condition for 2 wk. Bars, 10 μm.

(**3**) Transcriptional activation of Fe-deficiency responsive genes involved in Strategy II was suppressed in the *osbhlh156-1* mutant (Table 1).

(**4**) OsbHLH156 and IRO2 interact with each other (Fig. 5) and IRO2 was localised to the nucleus only in the presence of OsbHLH156 (Fig. 6).

Previous studies have shown that the bHLH transcription factor IRO2 is required for the expression of genes involved in Strategy II for Fe acquisition in rice (Ogo *et al.*, 2007). However, it is unknown how IRO2 regulates these genes, partly because the subcellular localisation of IRO2 has not been unambiguously determined. Our results indicated that OsbHLH156 and IRO2 are both required in rice to activate the expression of genes involved in Strategy II of Fe acquisition under Fe-deficient conditions, and that OsbHLH156 acts to localise IRO2 to the nucleus.

OsbHLH156 is orthologous to FER/FIT in Strategy I plant species although the amino acid sequence similarity between them is low (Fig. S1). In Arabidopsis, FIT protein interacts with clade Ib bHLH proteins (i.e. bHLH38/39/100/101) (Wang *et al.*, 2013; Yuan *et al.*, 2008) to regulate the downstream Fe-responsive genes, and our studies strongly indicated a similar mechanism in which OsbHLH156 interacted with the bHLH Ib family protein IRO2. By interacting with IRO2, OsbHLH156 acts as an essential regulator for the Strategy II Fe uptake in rice. Therefore, irrespective of the routes used by different plants for Fe uptake, that is Strategy I or II, the master regulator, OsbHLH156 or FIT, forms a functionally active heterodimeric complex with another bHLH transcription factor from the bHLH Ib subfamily. This type of interaction may exist widely in the Fe acquisition regulatory pathway in either Strategy I or Strategy II plants. This finding provides a novel insight into the evolution of Fe acquisition strategies in plants.

Our previous study showed that the *NAAT1* mutation, *naat1,* abolished MA synthesis in Strategy II (Cheng *et al.*, 2007). By stimulating Strategy I Fe uptake, the *naat1* plants grew even better than the wild-type when supplied with Fe(II). The reason for the better growth in *naat1* is mainly attributed to the overaccumulation of NA caused by lost function of the NAAT enzyme. NA is known as the important Fe chelator and participates in Fe phloem transport (Koike *et al.*, 2004). In the *osbhlh156* mutant, the expression of *NAS1/2* genes was undetected, and would abolish the synthesis of NA. Hence, the low Fe content in the *osbhlh156* mutant (Figs 2e, 4c, f) is attributed to the reduction of both Fe uptake via Strategy II and the efficiency to transport Fe taken by both strategies.

Global analyses of the transcriptomic responses of *osbhlh156-1* to Fe deficiency revealed that while the *osbhlh156-1* mutant induced a greater number of transcripts compared with the wild-type, < 10% of the genes overlapped with the changes in wild-type (Figs 3a, S4). Notably, there were a greater number of transcripts of non-Strategy II genes whose expression was altered in *osbhlh156-1* roots by Fe deficiency. These alterations might be due to the consequence of more severe Fe deficiency causing oxidative stress in *osbhlh156-1*. It is also possible that the dramatic changes in gene expression observed in *osbhlh156-1* could be due to OsbHLH156 interacting with other transcription factors that are involved in the response to Fe deficiency in a similar way as with IRO2, or that OsbHLH156 itself might be capable of acting as a transcription factor in the activation of gene expression in response to low Fe stress.

In conclusion, OsbHLH156, characterised here, is required to localise IRO2 to the nucleus, where IRO2 activates downstream genes involved in Strategy II Fe acquisition in rice.

Acknowledgements

The authors would like to thank Luis Herrera-Estrella of the Laboratorio Nacional de Genómica para la Biodiversidad (LANGEBIO), Mexico for providing productive discussion. We also thank Heven Sze (University of Maryland, College Park, MD, USA) and Mary Williams (Editor of The Plant Cell), for critical comments and manuscript editing. Shelong Zhang provided technical support in the use of fluorescence microscope in the study. This work was supported by the Ministry of Science and Technology of China (2016YFD0100703), the National Natural Science Foundation of China (31401934, 31572189 and 31771689), the Natural Science Foundation of Zhejiang Province (LZ16C 150001), the Ministry of Education (B14027), the Australian Research Council Centre of Excellence Program (Grant no. CE140100008), and by Grant-in-Aid for Specially Promoted Research (JSPS KAKENHI Grant no. 16H06296 to JFM).

Author contributions

SW and HS designed the project; SW performed the experiments together with LL, YY, JW, JFS and NY; SW, JW, JFM and HS analysed the data and wrote the article.

ORCID

Lin Li https://orcid.org/0000-0002-5532-4577
Jian Feng Ma https://orcid.org/0000-0003-3411-827X
Ji Feng Shao https://orcid.org/0000-0001-6712-8488
Huixia Shou https://orcid.org/0000-0001-6890-5672
Jin Wang https://orcid.org/0000-0002-7558-3808
Shoudong Wang https://orcid.org/0000-0002-1730-0267
James Whelan https://orcid.org/0000-0001-5754-025X
Naoki Yamaji https://orcid.org/0000-0002-7499-3004
Yinghui Ying https://orcid.org/0000-0002-7160-152X

References

Balk J, Schaedler TA. 2014. Iron cofactor assembly in plants. *Annual Review of Plant Biology* **65**: 125–153.

Bashir K, Inoue H, Nagasaka S, Takahashi M, Nakanishi H, Mori S, Nishizawa NK. 2006. Cloning and characterization of deoxymugineic acid synthase genes from graminaceous plants. *Journal of Biological Chemistry* **281**: 32395–32402.

Bauer P, Ling HQ, Guerinot ML. 2007. FIT, the FER-LIKE iron deficiency induced transcription factor in Arabidopsis. *Plant Physiology Biochemistry* **45**: 260–261.

Briat JF, Dubos C, Gaymard F. 2015. Iron nutrition, biomass production, and plant product quality. *Trends in Plant Science* **20**: 33–40.

Brumbarova T, Bauer P, Ivanov R. 2015. Molecular mechanisms governing Arabidopsis iron uptake. *Trends in Plant Science* **20**: 124–133.

Bughio N, Yamaguchi H, Nishizawa NK, Nakanishi H, Mori S. 2002. Cloning an iron-regulated metal transporter from rice. *Journal of Experimental Botany* **53**: 1677–1682.

Chen S, Jin W, Wang M, Zhang F, Zhou J, Jia Q, Wu Y, Liu F, Wu P. 2003. Distribution and characterization of over 1000 T-DNA tags in rice genome. *The Plant Journal* **36**: 105–113.

Cheng L, Wang F, Shou H, Huang F, Zheng L, He F, Li J, Zhao FJ, Ueno D, Ma JF, Wu P. 2007. Mutation in nicotianamine aminotransferase stimulated the Fe(II) acquisition system and led to iron accumulation in rice. *Plant Physiology* **145**: 1647–1657.

Colangelo EP, Guerinot ML. 2004. The essential basic helix–loop–helix protein FIT1 is required for the iron deficiency response. *Plant Cell* **16**: 3400–3412.

Curie C, Panaviene Z, Loulergue C, Dellaporta SL, Briat JF, Walker EL. 2001. Maize yellow stripe1 encodes a membrane protein directly involved in Fe(III) uptake. *Nature* **409**: 346–349.

Guerinot ML, Yi Y. 1994. Iron: Nutritious, noxious, and not readily available. *Plant Physiology* **104**: 815–820.

Higuchi K, Suzuki K, Nakanishi H, Yamaguchi H, Nishizawa NK, Mori S. 1999. Cloning of nicotianamine synthase genes, novel genes involved in the biosynthesis of phytosiderophores. *Plant Physiology* **119**: 471–480.

Inoue H, Higuchi K, Takahashi M, Nakanishi H, Mori S, Nishizawa NK. 2003. Three rice nicotianamine synthase genes, OsNAS1, OsNAS2, and OsNAS3 are expressed in cells involved in long-distance transport of iron and differentially regulated by iron. *The Plant Journal* **36**: 366–381.

Inoue H, Kobayashi T, Nozoye T, Takahashi M, Kakei Y, Suzuki K, Nakazono M, Nakanishi H, Mori S, Nishizawa NK. 2009. Rice OsYSL15 is an iron-regulated iron(III)-deoxymugineic acid transporter expressed in the roots and is essential for iron uptake in early growth of the seedlings. *Journal of Biological Chemistry* **284**: 3470–3479.

Ishimaru Y, Suzuki M, Tsukamoto T, Suzuki K, Nakazono M, Kobayashi T, Wada Y, Watanabe S, Matsuhashi S, Takahashi M, Nakanishi H, Mori S, Nishizawa NK. 2006. Rice plants take up iron as an Fe^{3+}-phytosiderophore and as Fe^{2+}. *The Plant Journal* **45**: 335–346.

Jakoby M, Wang HY, Reidt W, Weisshaar B, Bauer P. 2004. FRU (BHLH029) is required for induction of iron mobilization genes in *Arabidopsis thaliana*. *FEBS Letters* **577**: 528–534.

Kobayashi T, Nagasaka S, Senoura T, Itai RN, Nakanishi H, Nishizawa NK. 2013. Iron-binding haemerythrin RING ubiquitin ligases regulate plant iron responses and accumulation. *Nature Communications* **4**: 2792.

Kobayashi T, Ogo Y, Itai RN, Nakanishi H, Takahashi M, Mori S, Nishizawa NK. 2007. The transcription factor IDEF1 regulates the response to and tolerance of iron deficiency in plants. *Proceedings of the National Academy of Sciences, USA* **104**: 19150–19155.

Koike S, Inoue H, Mizuno D, Takahashi M, Nakanishi H, Mori S, Nishizawa NK. 2004. OsYSL2 is a rice metal-nicotianamine transporter that is regulated by iron and expressed in the phloem. *The Plant Journal* **39**: 415–424.

Korshunova YO, Eide D, Clark WG, Guerinot ML, Pakrasi HB. 1999. The IRT1 protein from *Arabidopsis thaliana* is a metal transporter with a broad substrate range. *Plant Molecular Biology* **40**: 37–44.

Lee S, Ryoo N, Jeon JS, Guerinot ML, An G. 2012. Activation of rice Yellow Stripe1-Like 16 (OsYSL16) enhances iron efficiency. *Molecules & Cells* **33**: 117–126.

Ling HQ, Bauer P, Bereczky Z, Keller B, Ganal M. 2002. The tomato fer gene encoding a bHLH protein controls iron-uptake responses in roots. *Proceedings of the National Academy of Sciences, USA* **99**: 13938–13943.

Ma JF, Nomoto K. 1996. Effective regulation of iron acquisition in graminaceous plants. The role of mugineic acids as phytoslderophores. *Physiologia Plantarum* **97**: 609–617.

Ma JF, Shinada T, Matsuda C, Nomoto K. 1995. Biosynthesis of phytosiderophores, mugineic acids, associated with methionine cycling. *Journal of Biological Chemistry* **270**: 16549–16554.

Nishida S, Tsuzuki C, Kato A, Aisu A, Yoshida J, Mizuno T. 2011. AtIRT1, the primary iron uptake transporter in the root, mediates excess nickel accumulation in *Arabidopsis thaliana*. *Plant & Cell Physiology* **52**: 1433–1442.

Nozoye T, Nagasaka S, Kobayashi T, Takahashi M, Sato Y, Sato Y, Uozumi N, Nakanishi H, Nishizawa NK. 2011. Phytosiderophore efflux transporters are crucial for iron acquisition in graminaceous plants. *Journal of Biological Chemistry* **286**: 5446–5454.

Ogo Y, Itai RN, Kobayashi T, Aung MS, Nakanishi H, Nishizawa NK. 2011. OsIRO2 is responsible for iron utilization in rice and improves growth and yield in calcareous soil. *Plant Molecular Biology* **75**: 593–605.

Ogo Y, Itai RN, Nakanishi H, Inoue H, Kobayashi T, Suzuki M, Takahashi M, Mori S, Nishizawa NK. 2006. Isolation and characterization of IRO2, a novel iron-regulated bHLH transcription factor in graminaceous plants. *Journal of Experimental Botany* **57**: 2867–2878.

Ogo Y, Itai RN, Nakanishi H, Kobayashi T, Takahashi M, Mori S, Nishizawa NK. 2007. The rice bHLH protein OsIRO2 is an essential regulator of the genes involved in Fe uptake under Fe-deficient conditions. *The Plant Journal* **51**: 366–377.

Ogo Y, Kobayashi T, Nakanishi Itai R, Nakanishi H, Kakei Y, Takahashi M, Toki S, Mori S, Nishizawa NK. 2008. A novel NAC transcription factor, IDEF2, that recognizes the iron deficiency-responsive element 2 regulates the genes involved in iron homeostasis in plants. *Journal of Biological Chemistry* **283**: 13407–13417.

Robinson NJ, Procter CM, Connolly EL, Guerinot ML. 1999. A ferric-chelate reductase for iron uptake from soils. *Nature* **397**: 694–697.

Rogers EE, Eide DJ, Guerinot ML. 2000. Altered selectivity in an Arabidopsis metal transporter. *Proceedings of the National Academy of Sciences, USA* **97**: 12356–12360.

Saleh A, Alvarez-Venegas R, Avramova Z. 2008. An efficient chromatin immunoprecipitation (ChIP) protocol for studying histone modifications in Arabidopsis plants. *Nature Protocols* **3**: 1018–1025.

Santi S, Schmidt W. 2009. Dissecting iron deficiency-induced proton extrusion in Arabidopsis roots. *New Phytologist* **183**: 1072–1084.

Takagi S. 1976. Naturally occurring iron-chelating compounds in oat- and rice-root washings. *Soil Science and Plant Nutrition* **22**: 423–433.

Takahashi M, Yamaguchi H, Nakanishi H, Shioiri T, Nishizawa NK, Mori S. 1999. Cloning two genes for nicotianamine aminotransferase, a critical enzyme in iron acquisition (Strategy II) in graminaceous plants. *Plant Physiology* **121**: 947–956.

Walker EL, Connolly EL. 2008. Time to pump iron: iron-deficiency-signaling mechanisms of higher plants. *Current Opinion in Plant Biology* **11**: 530–535.

Wang L, Ying Y, Narsai R, Ye L, Zheng L, Tian J, Whelan J, Shou H. 2013. Identification of OsbHLH133 as a regulator of iron distribution between roots and shoots in *Oryza sativa*. *Plant, Cell & Environment* **36**: 224–236.

Wang N, Cui Y, Liu Y, Fan H, Du J, Huang Z, Yuan Y, Wu H, Ling HQ. 2013. Requirement and functional redundancy of Ib subgroup bHLH proteins for iron deficiency responses and uptake in *Arabidopsis thaliana*. *Molecular Plant* **6**: 503–513.

Wang S, Yokosho K, Guo R, Whelan J, Ruan Y-L, Ma JF, Shou H. 2019. The soybean sugar transporter GmSWEET15 mediates sucrose export from endosperm to early embryo. *Plant Physiology* **180**: 2133–2141.

Wu H, Ling H-Q. 2019. FIT-binding proteins and their functions in the regulation of Fe homeostasis. *Frontiers Plant Science* **10**: doi: 10.3389/fpls.2019.00844.

Xie K, Minkenberg B, Yang Y. 2014. Targeted gene mutation in rice using a CRISPR-Cas9 system. *Bio-Protocol* **4**: e1225.

Yang X, Baliji S, Buchmann RC, Wang H, Lindbo JA, Sunter G, Bisaro DM. 2007. Functional modulation of the geminivirus AL2 transcription factor and silencing suppressor by self-interaction. *Journal of Virology* **81**: 11972–11981.

Ying Y, Yue W, Wang S, Li S, Wang M, Zhao Y, Wang C, Mao C, Whelan J, Shou H. 2017. Two h-type thioredoxins interact with the E2 ubiquitin conjugase PHO2 to fine-tune phosphate homeostasis in rice. *Plant Physiology* **173**: 812–824.

Yuan YX, Zhang J, Wang DW, Ling HQ. 2005. AtbHLH29 of *Arabidopsis thaliana* is a functional ortholog of tomato FER involved in controlling iron acquisition in strategy I plants. *Cell Research* **15**: 613–621.

Yuan Y, Wu H, Wang N, Li J, Zhao W, Du J, Wang D, Ling HQ. 2008. FIT interacts with AtbHLH38 and AtbHLH39 in regulating iron uptake gene expression for iron homeostasis in Arabidopsis. *Cell Research* **18**: 385–397.

Zheng L, Ying Y, Wang L, Wang F, Whelan J, Shou H. 2010. Identification of a novel iron regulated basic helix–loop–helix protein involved in Fe homeostasis in *Oryza sativa*. *BMC Plant Biology* **10**: 166.

Supporting Information

Additional Supporting Information may be found online in the Supporting Information section at the end of the article.

Fig. S1 Similarities among OsbHLH156, FIT and SlFER proteins.

Fig. S2 Protein sequence alignment of OsbHLH156 and its mutant forms.

Fig. S3 Characteristics of *osbhlh156-2* and *osbhlh156-3* mutants.

Fig. S4 Comparison in gene expression between wild-type and *osbhlh156-1* under Fe sufficient or deficient conditions.

Fig. S5 Expression of Fe-deficiency responsive genes in roots of wild-type, *osbhlh156-1* and the *osbhlh156-1* complementation plants under Fe-deficient and -sufficient conditions.

Fig. S6 Co-localisation of OsbHLH156 and IRO2 in the nucleus of protoplasts prepared from rice seedlings grown under Fe-replete conditions.

Table S1 Primers used in this study.

Table S2 Genes differentially expressed in the wild-type and *osbhlh156-1* mutant under Fe deficiency and sufficient conditions.

Table S3 Genes that displayed a reverse pattern of expression between wild-type and *osbhlh156-1* plants grown in Fe-deficient medium.

Please note: Wiley Blackwell are not responsible for the content or functionality of any Supporting Information supplied by the authors. Any queries (other than missing material) should be directed to the *New Phytologist* Central Office.